

PHOSPHORESCENCE MICROWAVE DOUBLE RESONANCE IN EXCITON STATES OF MOLECULAR CRYSTALS AND COHERENT STATES OF TRIPLET SPIN ENSEMBLES

C. B. HARRIS†

*Department of Chemistry, University of California, Berkeley,
and Inorganic Materials Research Division, Lawrence Berkeley Laboratory,
Berkeley, California 94720, USA*

ABSTRACT

Saturation of the zero-field electron spin transitions of a phosphorescent triplet state by a microwave field causes changes in the intensity and/or polarization of the emission and thus forms the basis for phosphorescence microwave double resonance (PMDR)‡ in excited triplet states. Because of the sensitivity of photon detection, the technique is capable of detecting as few as 10^4 molecules in a sample depending upon the details of the radiative channels being monitored. If phosphorescence is monitored from an exciton band, PMDR can be used to experimentally differentiate between diffusion limited exciton migration and migration describable by the group velocity of the wave packet of k states, i.e. coherent exciton migration. In the following paper the relationships between PMDR spectroscopy, coherent triplet exciton migration and density of states functions in molecular crystals will be illustrated for crystals which can be considered as models for one-dimensional excitons. In particular, a resonance theory will be outlined that incorporates explicitly exciton-phonon scattering into the Bloch equations and allows one to extract both the lifetime of a k state of the band and the coherence length of the exciton. PMDR experiments in 'one-dimensional' molecular crystals are presented which illustrate the salient features of the theory. The experimental results are interpreted using a statistical theory which explicitly includes the exciton band dispersion, the density of state function of band and trap states, and the group velocity of the exciton wave packets. From the above experiments, a coherence length between 300 and 10^4 Å and a coherence lifetime of 10^{-7} s have been found for k states in the centre of the band for certain substituted benzene crystals at 4 K.

Finally, some new PMDR methods for studying the coherent spin properties of mobile and non-mobile states based on optically detected electron spin echoes and echo trains in excited molecular states will be presented. Specifically, a technique will be presented that is capable of measuring any state of the coherence of the spin ensemble, regardless of the optical polarization of emission from the spin sublevels utilizing virtually all of the phosphorescence emission from excited states.

† Alfred P. Sloan Foundation Fellow.

‡ D. S. Tinti, M. A. El-Sayed, A. H. Maki and C. B. Harris, *Chem. Phys. Letters*, 3, 343 (1969).

1. INTRODUCTION

In order to experimentally differentiate between coherent and diffusion limited triplet Frenkel¹ exciton migration in molecular crystals one must specify both the coherence time associated with the wave vector k and the correlation time associated with the particular experimental approach used. For experiments utilizing a time-dependent oscillating field such as visible electromagnetic radiation at one extreme and a microwave field at the other, the experimental correlation time is in the order of the reciprocal frequency of the applied field. If the lifetime of an exciton k state is much longer than the experimental correlation time, excitons associated with individual k states may be experimentally investigated by the applied field. With this experimental imposition, it is clear why a complete description of the dynamics of exciton migration in the Frenkel limit which allows an experimental probe into the dynamics requires that the electronic states, the phonon states, and phonon-exciton coupling all be explicitly considered in terms of the crystal states. Indeed, it is the latter interaction that determines the primary mechanism responsible for electronic energy transfer in solids at both high and low temperatures and hence the nature of the experimental observables^{2,3}. At low temperature the density of phonon states becomes sufficiently small that scattering between the exciton wave vector states k by the phonons is expected to be much less frequent than the intermolecular exchange time. In the limit that the time between scattering events approaches the radiative or radiationless lifetime of the excited electronic state, a Frenkel exciton can be thought of as an excitation propagating coherently as a wave packet at a velocity characteristic of both its energy and the linear combination of crystal k states which describe the wave packet. This velocity is termed the group velocity and is given by:

$$V_g(k) = (2\pi/h) (d\varepsilon/dk) \quad (1)$$

For a one-dimensional crystal,

$$\varepsilon(k) = E^0 + 2\beta \cos ka \quad (2)$$

where $\varepsilon(k)$ is the band dispersion associated with translational equivalent interactions along a direction a . E^0 is the electronic energy of the localized molecular excited state while β is the effective intermolecular interaction in the nearest neighbour approximation. In a stochastic model the distance which an exciton propagates in a coherent fashion without changing either its direction or velocity, $l(k)$, is given by the lifetime of the coherent state, $\tau(k)$, times the group velocity of the wavepacket:

$$l(k) = V_g(k) \times \tau(k) \quad (3)$$

$l(k)$ is thus equivalent to a mean-free path and $\tau(k)$ corresponds to a correlation time for the wave vector state k or linear combination of k states at an energy $\varepsilon(k)$ associated with the zeroth order state. From a dynamical point of view the important feature of coherent migration is that excitons can propagate in the crystal at a variety of velocities and a variety of distances depending upon the k states populated. *Figure 1* illustrates a few of the important features associated with coherent migration.

PHOSPHORESCENCE MICROWAVE DOUBLE RESONANCE

Coherent properties of excitons

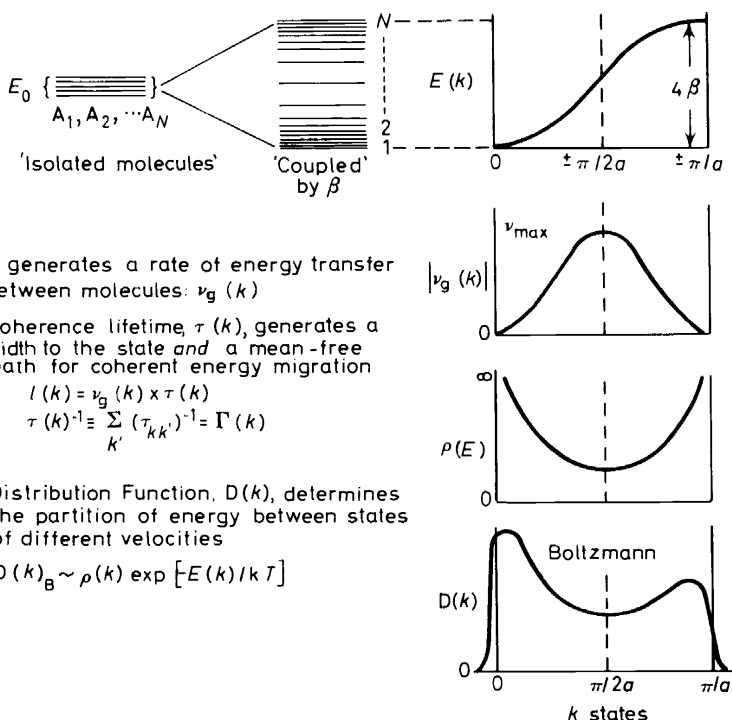


Figure 1. Experimental observables associated with coherent migration

When a thermal distribution characterizes the band, the number of excitons, $N(k)$, propagating with a velocity, $V_g(k)$, at a given temperature is proportional to the density of states $\rho(\varepsilon)$ times the Boltzmann factor.

$$N(k) = \frac{\rho(\varepsilon) \exp(-\varepsilon(k)/kT)}{\int \rho(\varepsilon) \exp(-\varepsilon(k)/kT)} \quad (4)$$

In the absence of damping or elastic scattering between $+k$ and $-k$ states, one can show that the wave vector states in the centre of the band can have velocities 10^6 – 10^7 times those associated with random walk migration for bands having dispersions between 1 and 10 cm^{-1} and that the coherence length can approach macroscopic dimensions if phonon–exciton scattering is weak (i.e. $\tau(k)$ is long) and the excited states are long-lived (e.g. triplet states). In practice this is only achieved in very pure crystals at low temperatures where the distribution of phonon states approaches the low-temperature limit. At intermediate temperatures the principal limitation of $\tau(k)$ is inelastic phonon–exciton scattering. In such cases an exciton initially at an energy $\varepsilon(k)$ scatters to other energies $\varepsilon(k')$ via phonon interactions in a time short compared to the radiative or radiationless lifetime, but in a time long

compared to intermolecular exchange. As a result the coherence time is shortened, the mean-free path or coherence length is reduced, and the individual k states acquire a width $\Gamma(k)$, given by the reciprocal of the coherence lifetime of the individual k states. $\Gamma(k)$ is given by

$$\Gamma(k) \equiv (\tau(k))^{-1} = \sum_k (\tau_{kk'})^{-1} \quad (5)$$

where $\tau_{kk'}$ is the probability of an exciton initially in an energy associated with the k th state scattering via phonon-exciton interactions to a final energy associated with the state k' .

In summary, a proper description of the dynamics of exciton migration must include in addition to the stationary states of the crystal (a) the group velocities of excitons, (b) the population distribution over the k states of the band, and (c) the coherence times for the individual k states and hence an explicit model for phonon-exciton scattering. This stochastic description views the exciton as executing a random walk migration in a time on the order of the coherence lifetime but allows for long-range propagation via coherent migration in between scattering events.

From an experimental point of view, this model requires that careful attention be given to the relationship between the correlation time associated with coherence and the time scale of the particular experimental approach being employed. If, for example, the experimental correlation time, which is on the order of the reciprocal of the radiation field, is much shorter than $\tau(k)$ (as is the case for optical absorption), only manifestations of the coherent model are apparent from the data. Similarly, when the experimental correlation time is longer than $\tau(k)$ for all k , only the random walk processes are displayed. A reliable measure of phenomena connecting coherent migration and diffusion limited migration, such as phonon-exciton scattering, $V_g(k)$ and $l(k)$, can only be determined when the experimental correlation time is on the order of $\tau(k)$. It is on this basis that electron spin resonance provides a direct probe into the dynamics of energy migration in triplet Frenkel excitons.

2. OPTICALLY DETECTED MAGNETIC RESONANCE IN COHERENT EXCITON STATES

In the absence of spin-orbit coupling the triplet band consists of three parallel spin-sublevel bands separated from one another by the zero-field electron spin dipolar interaction. This is illustrated in *Figure 2a*. In such a case, the microwave band-to-band electron spin transition (indicated by $\uparrow \downarrow$) is a single homogeneous line whose frequency is independent of the energy of the k states in the band. It has been shown⁴, however, that selective spin-orbit coupling between singlet bands and the individual triplet spin-sublevel bands results in a k dependence in the triplet exciton zero-field splitting as illustrated in *Figure 2a*. The net result is that a k dependent Larmor frequency, ω_0^k , which can be explicitly incorporated into the magnetic Bloch equations, allows different states in the band to be probed by either conventional electron spin resonance techniques or by optically detected magnetic resonance in which the change in the exciton phosphorescence, $h\nu$ (*Figure 2*), is monitored as a function of the microwave frequency (\uparrow). The line shape function for the

PHOSPHORESCENCE MICROWAVE DOUBLE RESONANCE

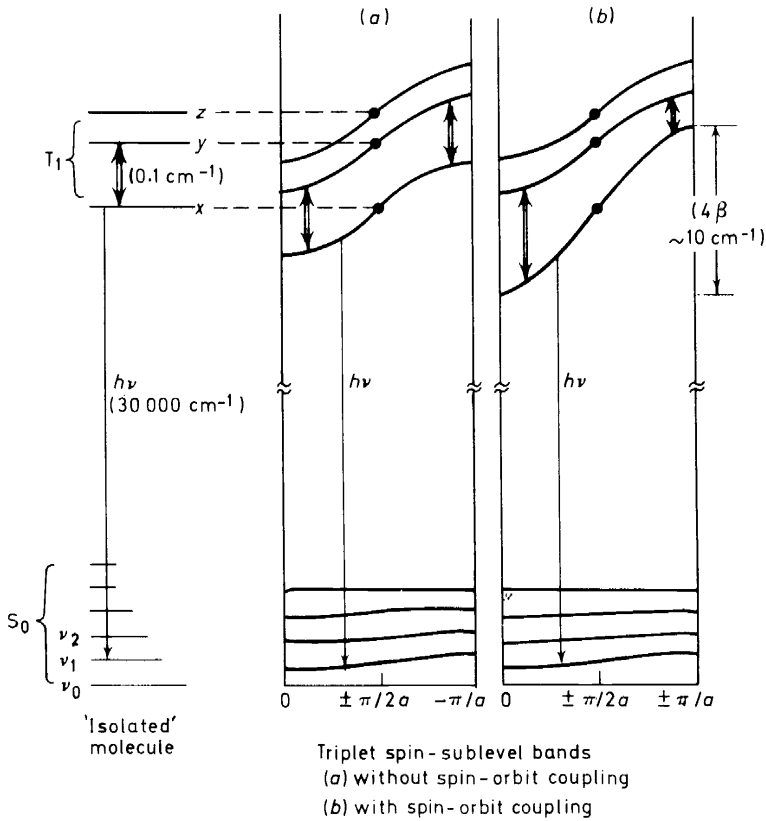


Figure 2. The magnetic spin sublevels in one-dimensional triplet bands

band-to-band electron-spin transitions can be solved in two limits. The first, termed the strong scattering case, occurs when $(\omega_0^k - \omega_0^{k'})\tau_{kk'} \ll 1$ and yields a homogeneously narrowed line centred at $k = \pm \pi/2a$ at high temperatures and corresponds to the random walk limit⁵. The second, when $(\omega_0^k - \omega_0^{k'})\tau_{kk'} \gg 1$, corresponds to the coherent limit in which phonon-exciton scattering causes a change in the exciton states on a time ($\tau_{kk'}$) slow compared to the differences in the Larmor frequencies ($\omega_0^k - \omega_0^{k'}$). In such cases the individual k states of the triplet band can be sampled by the rf field. Assuming phonon-exciton scattering to be uniform in k [$\tau(k)$ is uniform in k], the electron spin resonance absorption, $g(\omega)$, is the sum of $(2k + 1)$ independent Lorentz lines centred at ω_0^k and weighted by the number of excitons at energies $\epsilon(k)$ with a group velocity $V_g(k)$. The width of each Lorentz line has a contribution from both a finite coherence lifetime $\tau(k)$ and the homogeneous line with parameter $T_2(k)$. When a thermal distribution characterizes the triplet band

$$g(\omega) = \frac{\delta}{\pi} \int_0^{\pi/a} \frac{\exp[4\beta(1 - \cos ka)/kT]}{[\omega + \Delta_{ST}^k \cos ka]^2 + \delta^2} dk \quad (6)$$

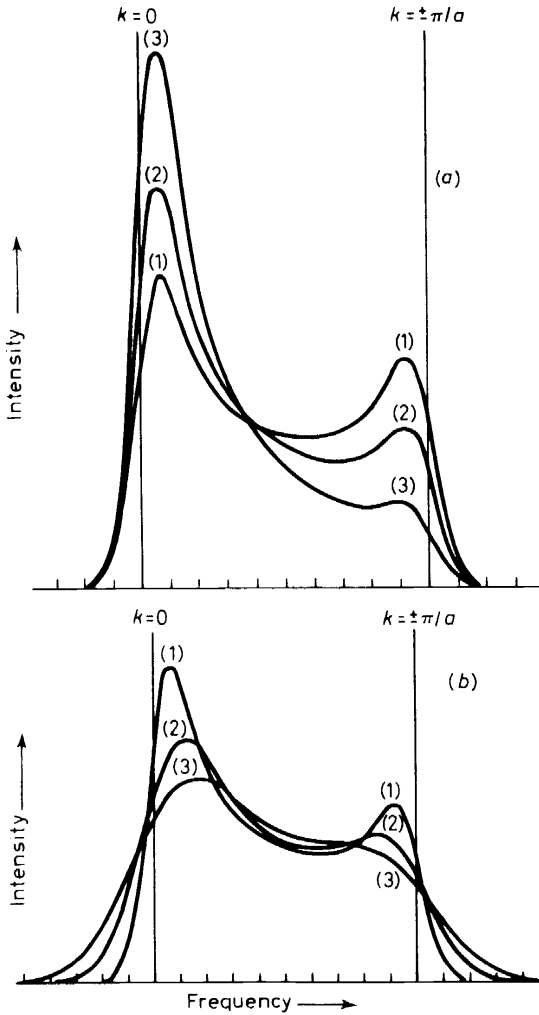


Figure 3. Microwave line shape profiles for electron spin band-to-band transitions in the coherent limit

Δ_{ST}^{ξ} is related to spin-orbit coupling⁴. T is temperature. δ is the half-width at half-height of an individual k state electron spin transition and is a measure of $\tau(k)$.

Some specific features of equation 6 are that: (a) the Larmor frequencies are directly related to band energy insofar as a prescribed ω_0^k couples the spin sublevels of an exciton whose energy is $\varepsilon(k)$; (b) the intensity of the transition is directly related to the density of states function times a Boltzmann factor. Thus, both the distribution function over the k states and hence the bandwidth are experimentally obtained⁶. (c) The broadening function, δ , gives an estimate of the phonon-exciton scattering, and hence a measure of

the coherence length, $l(k)$, and insight into the mechanism of phonon-exciton scattering. (d) The overall width of the transition is determined by the spin-orbit coupling parameter, Δ_{ST}^{ξ} , hence the selectivity of spin-orbit coupling to the triplet spin sublevels can be determined. (e) The microwave field selectivity perturbs the electron spin of excitons whose group velocity is $V_g(k)$, and therefore, the k dependence of other processes such as the dynamics of trapping^{7,8}, exciton-exciton annihilation, etc., can be potentially studied in the coherent limit. A few of these features are illustrated in *Figure 3*. Assuming the coherence lifetime $\tau(k)$ is the same for all states in the band. *Figure 3a* illustrates the line shape profile as a function of the bandwidth to temperature ratio, $4\beta/T$. Curves (1), (2) and (3) in *Figure 3a* are associated with $4\beta/T$ equal to 0.25, 0.75 and 1.5, respectively. The dependence on the coherence lifetime, $\tau(k)$, is illustrated in *Figure 3b*. Curves (1), (2) and (3) are associated with $\tau(k)^{-1}$ equal to 0.10, 0.18 and 0.26 times 4β . All curves in *Figure 3* assume a Boltzmann distribution in the triplet band.

Crystals in which the largest intermolecular exchange interaction is between translationally equivalent molecules can be considered models for one-dimensional crystals. The phosphorescence microwave double resonance results for the band-to-band transitions found in 1,2,4,5-tetrachlorobenzene are illustrated in *Figures 4a* and *4b*. Details of these experiments have been reported earlier⁶.

In the context of the above theoretical model, analysis of the data yields the following information about the lowest triplet exciton state in this pseudo 'one-dimensional' crystal. First, the bandwidth is about 1.3 cm^{-1} ⁶ and the $k = 0$ state is at the top of the band⁹. Secondly, the coherence lifetime of the k states is about 10^{-7} s. Finally, all k states have about the same coherence lifetime, implying the lack of strong k dependent phonon-exciton scattering at 4.2 K. If localization of the band states^{10,11} via mixing of the + and - wave vector states (elastic damping) is less than localization via inelastic processes such as phonon-exciton scattering, a coherence time of 10^{-7} s could allow coherent exciton migration to propagate as far as 10^4 \AA for states in the centre of the band ($k = \pm\pi/2a$) in these crystals. On the other hand, elastic damping could greatly reduce this coherence length⁸. Unfortunately, the Larmor frequencies for $+k$ and $-k$ states, ω_0^k and ω_0^{-k} , are the same, and hence, the above experiments cannot detect the effects of elastic scattering or damping. From other experiments^{7,8}, however, which will not be presented here, a lower limit on the coherence length in these crystals for $k = \pm\pi/2a$ of 300 \AA - 400 \AA has been determined.

In view of the importance of the exciton band-to-band line shape broadening function in the interpretation of properties associated with coherence energy migration in triplet excitons, it is desirable to have an experimental method capable of investigating the homogeneous character of the electron spin transitions. The homogeneous line width can be directly related to the lifetime of the states when other contributions to the line width, such as fluctuating local fields, are negligible compared to uncertainty broadening. It is also desirable to develop techniques which allow us to observe the dynamics of localized and delocalized excited states utilizing the sensitivity associated with phosphorescence microwave double resonance. Finally, the techniques should allow the full correlation function for the dynamical

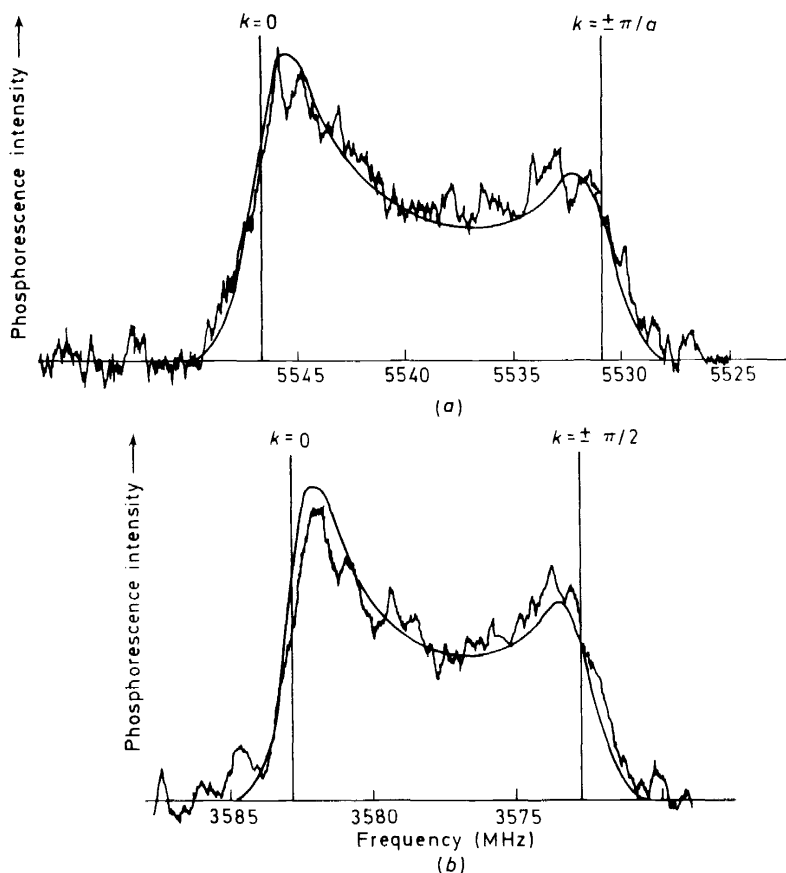


Figure 4. Observed zero-field band-to-band transitions at 4 K for 1,2,4,5-tetrachlorobenzene: (a) $D + |E\rangle$ transition. (b) $D - |E\rangle$ transition

processes to be obtained. All of these requirements are satisfied by the optical detection of electron spin echo trains where the Fourier transform of the decay of the echo train measured as a function of the time between echoes (2τ) is related to the line-shape function for the effective relaxation processes.

In the remainder of this paper, a general technique of optically detecting phenomena in solids that contribute to the dephasing of the ensemble of electron spins in excited triplet states will be presented although specific application of these techniques to coherent energy migration will be deferred to another publication.

3. OPTICALLY DETECTED ELECTRON SPIN ECHOES AND ECHO TRAINS IN MOLECULAR EXCITED TRIPLET STATES

Triplet states in zero-field can be viewed¹² in an interaction representation which removes the electron-spin zero-field Hamiltonian. In the rotating

PHOSPHORESCENCE MICROWAVE DOUBLE RESONANCE

frame a pseudomagnetization M_z is related to individual spin-sublevel populations in the laboratory frame. Population in each of the two zero-field spin sublevels being coupled by the applied field are associated with 'magnetization' along $+z$ and $-z$ in the interaction representation, respectively. When the time-dependent density matrix describing the zero-field spins is displayed through the electric dipole transition moment responsible for phosphorescence, usually only changes in $+$ and $-$ components along the z axis in the interaction representation are related to a modulation of the phosphorescence intensity¹². To overcome this limitation and optically detect phasing or dephasing phenomena, such as electron spin echoes¹³ which occur in the x,y -plane, a $\pi/2$ pulse can be applied at various times at the end of a normal pulse experiment¹⁴ in order to restore population to the z axis and observe the resulting change in phosphorescence intensity. The net result is that spin echoes¹³, spin echo trains¹⁵, spin locking¹⁶, and other coherent electron spin experiments can be detected optically^{14,17} on as few as 10^4 spins by restoring the spin ensemble from the x,y -plane to the $\pm z$ axis and observing the resulting change in phosphorescence as it reflects the instantaneous spin coherence in the interaction representation x,y -plane. The sensitivity of this method is only limited by the sensitivity of photon detection since virtually all of the phosphorescence intensity can be utilized to detect the echo. *Figure 5* compares the change in the phosphorescence

Optically detected electron spin echo
in the $^3\pi\pi^*$ state of h_2 -TCB (Y-trap)

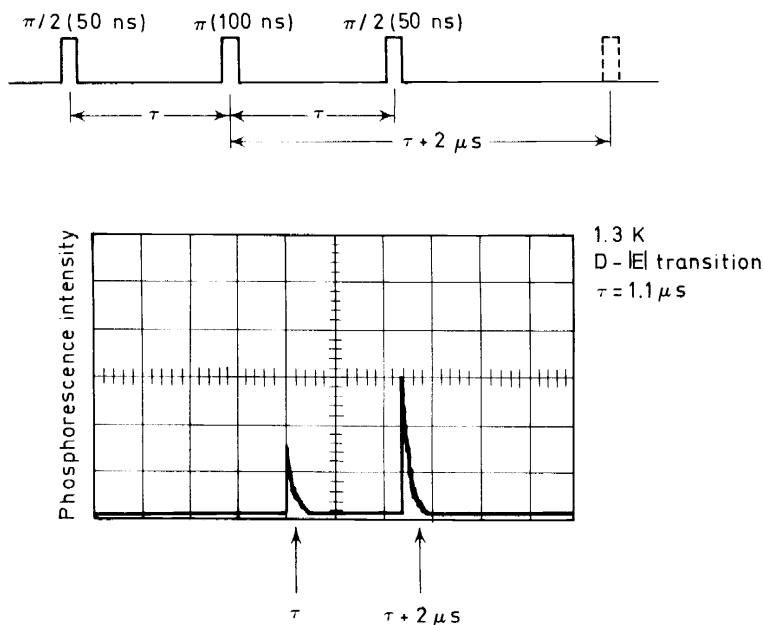


Figure 5. Phosphorescence intensity when spin coherence is rephased in the echo (τ) and when the spin ensemble is completely dephased ($\tau + 2 \mu s$)

intensity from the Y-trap of h_2 -TCB when the final $\pi/2$ pulse is applied at precisely the point where the echo is forming in time (τ) and at a point where the electron spins are completely dephased ($\tau + 2\mu\text{s}$). Details of the experiments will be presented elsewhere¹⁸. The homogeneous line width can be obtained by a plot of the Hahn echo¹³ amplitude versus 2τ . T_2 found for h_2 -TCB (Y-trap) was only $8\ \mu\text{s}$. The dephasing of the electron spins in this experiment is associated with a time corresponding to the fluctuations of local fields due to nuclear spins in the lattice on molecules adjacent to the excited state. In order to observe the dynamics of phenomena correlated to the electron spins for times longer than a few microseconds, it is necessary to remove the contribution to the electron T_2 from nuclear spin flips in the bulk solid since these limit T_2 to nuclear spin diffusion times (microseconds). This is accomplished by the continuous application of a microwave field of sufficient strength to ensure that the resonant frequency in the rotating frame, γH_1 , is large compared to electron-nuclear coupling¹⁷. In such cases, the homogeneous T_2 of the 'decoupled' electron spins can be obtained by the optical detection of rotary spin echoes¹⁷. This is schematically illustrated in *Figure 6* where the relationship of the rotating frame pseudomagnetization vector to the laboratory frame spin-sublevel population in the triplet state is depicted.

Optically detected rotary echoes in excited triplet states

(Relationship between the laboratory frame and the interaction representation)

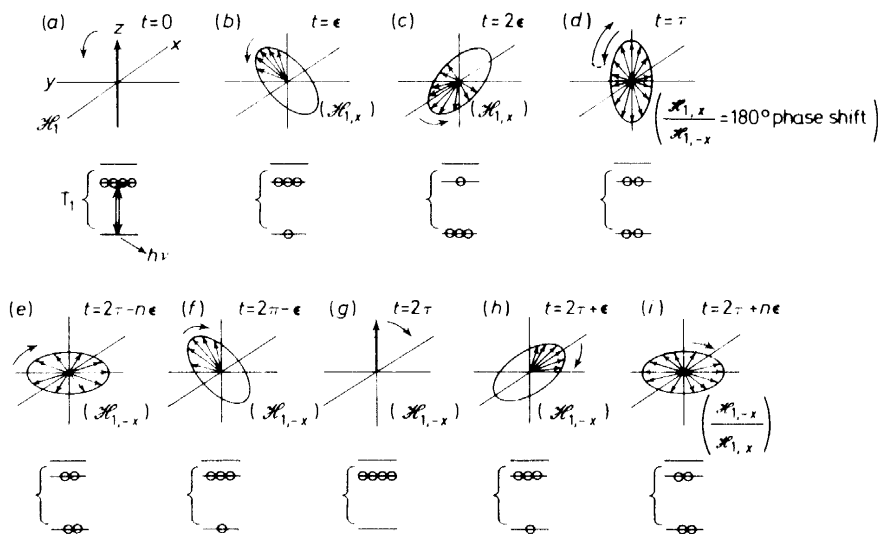


Figure 6. The relationship of the laboratory frame populations in the spin sublevels and the rotating frame magnetization in a rotary echo

A microwave H_1 field is continuously applied throughout the train; however, its phase is shifted by 180° at times $\tau, 3\tau, 5\tau, \dots$ leading to the resultant formation of echoes at times $2\tau, 4\tau, 6\tau, \dots$. An advantage of rotary echoes particularly suited to optical detection is the fact that the echoes

PHOSPHORESCENCE MICROWAVE DOUBLE RESONANCE

form along z in the rotating frame, and thus their amplitudes are directly related to the zero-field spin-sublevel populations of the triplet state in the laboratory frame and hence to the phosphorescence intensity. In the echo train, the amplitude decays in the rotating frame with a decay constant $T_{2\rho}$ which can be a sensitive function of τ . Part of an optically detected rotary echo train illustrated in *Figure 7* for the $^3\pi\pi^*$ state of tetrachlorobenzene¹⁷. In our measurements in the above excited state, $T_{2\rho}$ was found to

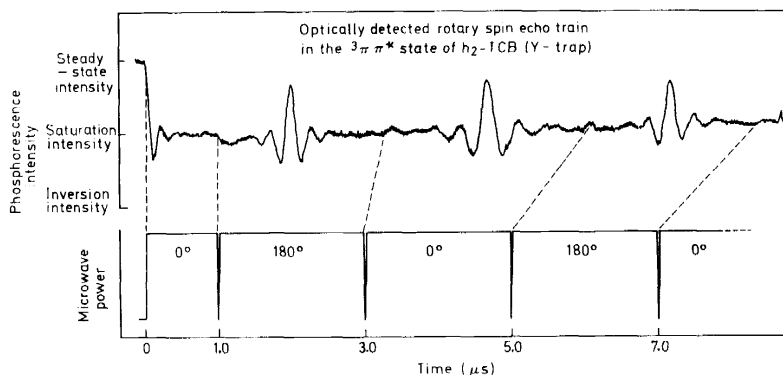


Figure 7. Optically detected rotary echo train

be $\sim 600 \mu\text{s}$ for a $\tau = 1 \mu\text{s}$. In addition, $T_{2\rho}$ was found to vary significantly with τ , presumably because of energy migration between traps in these crystals⁷.

The importance of these techniques to the study of exciton migration, detrapping and other phenomena associated with molecular crystals is that they provide in principle a method of extracting the full correlation function for the dephasing of the electron spin ensemble. The correlation function is simply related to the Fourier transform of $T_{2\rho}$ versus 2τ . Because different phenomena such as coherent versus incoherent migration, trapping and detrapping, dephase the electron spins with dramatically different correlation times, the contribution of each can be determined from the Fourier spectrum of the electron spin relaxation function.

4. ACKNOWLEDGEMENTS

This work was supported in part by the National Science Foundation and in part by the US Atomic Energy Commission.

Finally, I would like to thank the Soviet and Estonian Academies of Science for the invitation and support in presenting this paper before such a distinguished audience in the fields of molecular crystals and magnetic resonance at the XIth European Congress on Molecular Spectroscopy.

REFERENCES

- ¹ J. Frenkel. *Phys. Rev.*, **37**, 17, 1276 (1931); A. S. Davydov. *Theory of Molecular Excitons*. McGraw-Hill. New York (1962).
- ² T. Holstein. *Ann. Phys. (New York)*, **8**, 343 (1959); M. Grover and R. Silbey. *J. Chem. Phys.*, **54**, 4843 (1971).
- ³ R. W. Munn and W. Siebrand. *J. Chem. Phys.*, **52**, 47 (1970).
- ⁴ A. H. Francis and C. B. Harris. *Chem. Phys. Letters*, **9**, 181 (1971).
- ⁵ Z. G. Soos and H. M. McConnell. *J. Chem. Phys.*, **43**, 3780 (1965).
- ⁶ A. H. Francis and C. B. Harris. *Chem. Phys. Letters*, **9**, 188 (1971).
- ⁷ A. H. Francis and C. B. Harris. *J. Chem. Phys.*, **55**, 3595 (1971).
- ⁸ M. D. Fayer and C. B. Harris. *Phys. Rev.*, **B9**, 748 (1974).
- ⁹ M. D. Fayer. A. H. Francis and C. B. Harris. unpublished results.
- ¹⁰ G. F. Koster and J. C. Slater. *Phys. Rev.*, **95**, 1167 (1954), **96**, 1208 (1954).
- ¹¹ E. I. Rashba. *Opt. Spectr.*, **2**, 568 (1957); D. P. Craig and M. R. Philpott. *Proc. Roy. Soc.*, **A290**, 583, 602; **A293**, 213 (1966); H.-K. Hong and G. W. Robinson. *J. Chem. Phys.*, **52**, 825 (1970); H.-K. Hong and R. Kopelman. *J. Chem. Phys.*, **55**, 5380 (1971).
- ¹² C. B. Harris. *J. Chem. Phys.*, **54**, 972 (1971).
- ¹³ E. L. Hahn. *Phys. Rev.*, **80**, 580 (1950).
- ¹⁴ W. G. Breiland, C. B. Harris and A. Pines. *Phys. Rev. Letters*, **30**, 158 (1973).
- ¹⁵ H. Y. Carr and E. M. Purcell. *Phys. Rev.*, **94**, 630 (1954).
- ¹⁶ A. G. Redfield. *Phys. Rev.*, **98**, 1787 (1955); I. Solomon. *C. R. Acad. Sci. Paris*, **248**, 92 (1959).
- ¹⁷ C. B. Harris, R. L. Schlupp and H. Schuch. *Phys. Rev. Letters*, **30**, 1010 (1973).
- ¹⁸ W. G. Breiland and C. B. Harris. unpublished results.